Inorganic Chemistry
Article

Inorg. Chem. **2010**, *49*, 2557–2567 **2557**
DOI: 10.1021/ic902531p

Does the MgO(100)-Support Facilitate the Reaction of Nitrogen and Hydrogen Molecules Catalyzed by Zr_2Pd_2 Clusters? A Computational Study

Aleksey E. Kuznetsov and Djamaladdin G. Musaev*

Cherry L. Emerson Center for Scientific Computation, Emory University, 1515 Dickey Drive, Atlanta, Georgia 30322

Received December 18, 2009

Reactions of the "naked" and MgO(100) supported Zr_2Pd_2 cluster with nitrogen and four hydrogen molecules were studied at the density functional level using the periodic slab approach (VASP). It was shown that adsorption of the Zr_2Pd_2 cluster on the MgO(100) surface does not change its gas-phase geometry and electronic structure significantly. In spite of this the N_2 coordination to the MgO(100)-supported Zr_2Pd_2 cluster, **I/MgO**, is found to be almost 30 kcal/mol less favorable than for the "naked" one. The addition of the first H_2 molecule to the resulting **II/MgO**, that is, **II/MgO** + $H_2 \rightarrow$ **IV/MgO** reaction, proceeds with a relatively small, 9.0 kcal/mol, barrier and is exothermic by 8.3 kcal/mol. The same reaction for the "naked" Zr_2Pd_2 cluster requires a slightly larger barrier (10.1 kcal/mol) and is highly exothermic (by 23.3 kcal/mol). The interaction of the H_2 molecule with the intermediate **IV/MgO** (i.e., the second H_2 molecule addition to **II/MgO**) requires larger energy barrier, 23.3 kcal/mol vs 8.8 kcal/mol for the "naked" cluster, and is exothermic by 20.5 kcal/mol (vs 18.2 kcal/mol reported for the "naked" Zr_2Pd_2 cluster). The addition of the H_2 molecule to **VI/MgO** and **VI** (i.e., the third H_2 molecule addition to **II/MgO** and **II**, respectively) requires similar barriers, 12.0 versus 16.8 kcal/mol, respectively, but is highly exothermic for the supported cluster compared to the "naked" one, 13.6 versus 0.1 kcal/mol. The addition of the fourth H_2 molecule occurs with almost twice larger barrier for the "naked" cluster compared to the adsorbed species, 30.7 versus 15.9 kcal/mol. Furthermore, this reaction step is endothermic (by 11.4 kcal/mol) for the gas-phase cluster but exothermic by 7.8 kcal/mol for the adsorbed cluster. Dissociation of the formed hydrazine molecule from the on-surface complex **X/MgO** and the "naked" complex **X** requires 19.1 and 26.3 kcal/mol, respectively. Thus, the Zr_2Pd_2 adsorption on the MgO(100) surface facilitates its reaction with N_2 and four H_2 molecules, as well as formation of hydrazine from the hydrogen and nitrogen molecules. The reported differences in the reactivity of the "naked" and MgO adsorbed Zr_2Pd_2 clusters were explained by analyzing the nature of the H_2 addition steps in these systems.

I. Introduction

Reduced nitrogen is an essential component of nucleic acids and proteins. The major part of all the nitrogen required in human nutrition is still obtained by biological nitrogen fixation. Nature has found a way to convert the inert nitrogen molecule to a useable form like ammonia under mild conditions using a small but diverse group of diazotrophic microorganisms that contain the enzyme nitrogenase.[1] The industrial analog of the nitrogenase, in terms of N≡N triple bond utilization, is the old Haber−Bosch[2] process. This heterogeneous process utilizes the Fe-particles with added potassium hydroxide on a support of alumina and silica as a catalyst to produce ammonia from the nitrogen and hydrogen molecules. As pointed out by Ertl,[3] fixation of N_2 by H_2 in this heterogeneous catalytic process occurs via the formation of atomic nitrogen and hydrogen on the surface (via the on-surface atomization of the N_2 and H_2 molecules) followed by the addition of H-atoms to the coordinated nitrogen to form ammonia. The atomization of N_2 on the surface was shown to be a slow step of the entire catalytic cycle. Empirically it had been found that the presence of potassium ions in the catalyst improves the efficiency of the process and is believed to promote the N≡N triple bond activation of the coordinated nitrogen molecule.

While the heterogeneous Haber−Bosch catalyst is robust, it operates at high temperature and pressure, and is less energy- and atom-efficient. Therefore, during the past several decades, chemists have been actively looking for soluble

*To whom correspondence should be addressed. E-mail: dmusaev@emory.edu.

(1) (a) Eady, R. R. *Perspectives on Bioinorganic Chemistry*; JAI Press: Greenwich, CT, 1991; p 255. (b) Kim, J.; Rees, D. C. *Nature* **1992**, *360*, 553–560. (c) Kim, J.; Rees, D. C. *Science* **1992**, *257*, 1667–1682. (d) Chan, M. K.; Kim, J.; Rees, D. C. *Science* **1993**, *260*, 792.

(2) (a) Smil, V. *Enriching the Earth: Fritz Haber, Carl Bosch, and the Tranformation of World Food Production*; The MIT Press: Boston, MA, 2001. (b) Ertl, G. *Chem. Rec.* **2001**, *1*, 33–45. (c) Schlogl, R. *Angew. Chem., Int. Ed.* **2003**, *42*, 2004–2008.

(3) Ertl, G. *Angew. Chem., Int. Ed.* **2008**, *47*, 3524–3535.

Published on Web 02/03/2010

Scheme 1. Possible Coordination Modes of the Nitrogen Molecule in the Mono- and Dinuclear Complexes

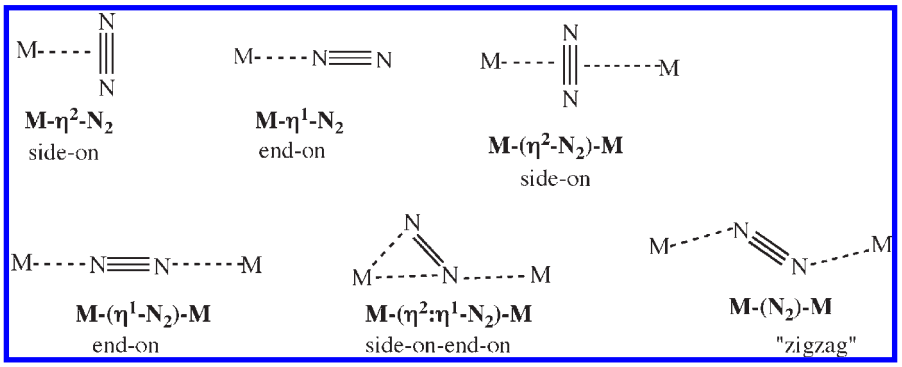

homogeneous version of the Haber−Bosch process that will (a) be more energy- and atom-efficient, (b) occur at the milder experimental conditions, and (c) be amenable to study and optimization. To this end, the extensive studies have led to the discovery of many fascinating new classes of homogeneous nitrogen fixation processes and elementary reactions. Currently much more accurate knowledge has been accumulated on the elementary steps and fundamental principles of N≡N triple bond activation and transformation. Many of these reactions have been extensively reviewed.[4−13]

It is well established that the first step of all the reported reactions is the dinitrogen coordination to a transition metal center of catalyst. It is shown that, in general, the N_2 molecule may coordinate to transition metal center(s) via several different ways (see Scheme 1), and be converted to ammonia (or its lower derivatives) via either protonation-reduction (known as Chatt mechanism)[14] or direct hydrogenation mechanisms (by direct addition of H_2 to the coordinated N_2). In the majority of the reported monotransition metal complexes of N_2 the latter is coordinated to the metal center in end-on (η^1) manner, which usually facilitates the formation of ammonia via the Chatt mechanism. However, the side-on (η^2-manner) or side-on-end-on (η^2:η^1-manner) coordination of N_2 to transition metal center(s) with strong M−N_2 interaction(s), which facilitates its direct hydrogenation (see Scheme 1), can be achieved in multitransition metal systems (complexes and small clusters). The exception is the complex $[(\eta^5\text{-}C_9H_5\text{-}1\text{-}^i\text{Pr-}3\text{-Me})_2\text{Zr-NaX}]_2(N_2)$ (where X = Cl, Br and I) reported by Chirik and co-workers,[15] where N_2 ligand is sandwiched between the Zr-centers, in the end-on fashion, and between Na ions, in the side-on fashion. Here the Na ions, most likely, play the same role as the potassium ions in Haber−Bosch catalyst.

Recently, we have shown[16] that the Zr_2Pd_2 and Zr_2Pt_2 clusters might be even more reactive than the reported dimeric Zr and Ta complexes.[6,11,13]

However, the use of these "naked" transition metal clusters in real experiments could be problematic, and, therefore, one should search for ways to stabilize them. One such way is to embed these clusters on the metal oxide surfaces. Gates and co-workers have demonstrated the experimental viability of such an approach.[17] However, the interaction of the embedded cluster with surface atoms may significantly alter the geometry, electronic structure, and reactivity of the free (free from the support) clusters. Therefore, to elucidate the effect of the surface-cluster interactions on the catalytic activity of the "naked" Zr_2Pd_2 cluster for the dinitrogen hydrogenation, below we embed it on the MgO(100) surface, the resulting system called as Zr_2Pd_2/MgO(100), and study the dinitrogen hydrogenation catalyzed by the free and embedded Zr_2Pd_2 cluster. Here we chose the MgO(100) surface because it is one of the most well-studied metal oxide surfaces and widely used as a support for metal clusters and nanoparticles.[18−30]

(4) (a) Leigh, G. J. *Acc. Chem. Res.* **1992**, *25*, 177−181 and references therein. (b) Leigh, G. J. *Science* **1998**, *279*, 506–507.
(5) Eady, R. R. *Chem. Rev.* **1996**, *96*, 3013–3030.
(6) (a) Fryzuk, M. D.; Love, J. B.; Rettig, S. J.; Young, V. G. *Science* **1997**, *275*, 1445–1447. (b) Fryzuk, M. D. *Acc. Chem. Res.* **2009**, *42*, 127–133. (c) MacKay, B. A.; Fryzuk, M. D. *Chem. Rev.* **2004**, *104*, 385–401.
(7) Nishibayashi, Y.; Iwai, S.; Hidai, M. *Science* **1998**, *279*, 540–542.
(8) (a) Basch, H.; Musaev, D. G.; Morokuma, K.; Fryzuk, M. D.; Love, J. B.; Seidel, W. W.; Albinati, A.; Koetzle, T. F.; Klooster, W. T.; Mason, S. A.; Eckert, J. *J. Am. Chem. Soc.* **1999**, *121*, 523–528. (b) Basch, H.; Musaev, D. G.; Morokuma, K. *J. Am. Chem. Soc.* **1999**, *121*, 5754–5761. (c) Basch, H.; Musaev, D. G.; Morokuma, K. *Organometallics* **2000**, *19*, 3393–3403. (d) Musaev, D. G.; Basch, H.; Morokuma, K. In *Computational Modeling of Homogeneous Catalysis*; Maseras, F., Lledos, A., Eds.; Kluwer Academic Publ.: Norwell, MA, 2002; pp 325−361. (e) Bobadova-Parvanova, P.; Wang, Q.; Morokuma, K.; Musaev, D. G. *Angew. Chem., Int. Ed.* **2005**, *44*, 7101–7103. (f) Yates, B. F.; Basch, H.; Musaev, D. G.; Morokuma, K. *J. Chem. Theory Comput.* **2006**, *2*, 1298–1316.
(9) Peters, J. C.; Cherry, J.-P. F.; Thomas, J. C.; Baraldo, L.; Mindiola, D. J.; Davis, W. M.; Cummins, C. C. *J. Am. Chem. Soc.* **1999**, *121*, 10053–10067.
(10) (a) Yandulov, D. M.; Schrock, R. R. *Science* **2003**, *301*, 76–78. (b) Yandulov, D. M.; Schrock, R. R. *Inorg. Chem.* **2005**, *44*, 1103–1117. (c) Yandulov, D. M.; Schrock, R. R.; Reingold, A. L.; Ceccarelli, C.; Davis, W. M. *Inorg. Chem.* **2003**, *42*, 796–813. (d) Ritleng, V.; Yandulov, D. M.; Weare, W. W.; Schrock, R. R.; Hock, A. S.; Davis, W. M. *J. Am. Chem. Soc.* **2004**, *126*, 6150–6163.
(11) (a) Pool, J. A.; Lobkovsky, E.; Chirik, P. J. *Nature* **2004**, *427*, 527–530. (b) Knobloch, D. J.; Lobkovsky, E.; Chirik, P. J. *Nature Chem.* **2010**, *2*, 30–35, and references therein. (c) Pool, J. A.; Bernskoetter, W. H.; Chirik, P. J. *J. Am. Chem. Soc.* **2004**, *126*, 14326–14327. (d) Hanna, T. E.; Lobkovsky, E.; Chirik, P. J. *J. Am. Chem. Soc.* **2004**, *126*, 14688–14689.
(12) Ding, K.; Pierpont, A. W.; Brennessel, W. W.; Lukat-Rodgers, G.; Rodgers, K. R.; Cundari, T. R.; Bill, E.; Holland, P. L. *J. Am. Chem. Soc.* **2009**, *131*, 9471–9472, and references therein.
(13) Hirotsu, M.; Fontaine, P. P.; Epshteyn, A.; Zavalij, P. Y.; Sita, L. R. *J. Am. Chem. Soc.* **2007**, *129*, 9284–9285.
(14) (a) Chatt, J.; Dilworth, J. R.; Richards, R. L. *Chem. Rev.* **1978**, *78*, 589–625. (b) Chatt, J. In *Nitrogen Fixation*; Stewart, W. D. P., Gallon, J. R. Eds.; Academic Press: New York, 1980; p 1.
(15) Pun, D.; Lobkovsky, E.; Chirik, P. J. *J. Am. Chem. Soc.* **2008**, *130*, 6047–6054.
(16) Musaev, D. G. *J. Phys. Chem. B* **2004**, *108*, 10012–10018.
(17) (a) Uzun, A.; Gates, B. C. *J. Am. Chem. Soc.* **2009**, *131*, 15887–15894. (b) Xu, Z.; Xiao, F.-S.; Purnell, S. K.; Alexeev, O.; Kawi, S.; Deutsch, S. E.; Gates, B. C. *Nature* **1994**, *372*, 346–348. (c) Argo, A. M.; Odzak, J. F.; Lai, F. S.; Gates, B. C. *Nature* **2002**, *415*, 623–626. (d) Argo, A. M.; Odzak, J. F.; Gates, B. C. *J. Am. Chem. Soc.* **2003**, *125*, 7107–7115.
(18) Bonacic-Koutecky, V.; Bürgel, C.; Kronik, L.; Kuznetsov, A. E.; Mitric, R. *Eur. Phys. J. D* **2007**, *45*, 471–476.
(19) Gleitsmann, T.; Vaida, M. E.; Bernhardt, T. M.; Bonacic-Koutecky, V.; Bürgel, C.; Kuznetsov, A. E.; Mitric, R. *Eur. Phys. J. D* **2007**, *45*, 477–483.
(20) Bosko, S. I.; Moskaleva, L. M.; Matveev, A. V.; Rösch, N. *J. Phys. Chem. A* **2007**, *111*, 6870–6880.

II. Calculation Procedures

To describe the ionic MgO(100) surface, we used the periodic approach, as implemented in the Vienna ab initio simulation package (VASP, version 4.6).[31−34] In this approach, the MgO(100) surface is modeled by periodically repeated four layer slab, with p(4 × 4) supercell containing 32 Mg and 32 O atoms. The supercell has dimensions $a = b =$ 8.42 Å and $c = 21.32$ Å, which includes a vacuum region of thickness of about 15 Å to guarantee no interactions between the slabs. The periodic supercell DFT calculations are performed using a plane wave basis set[35] in conjunction with ultrasoft pseudopotentials[36] and the gradient-corrected PW91 exchange-correlation functional as implemented in the VASP code. This approach will be further referred to as "PW91/US-PP." A 400 eV kinetic energy cutoff allowing convergence to 1×10^{-4} eV in total energy is used. The Brillouin zone is sampled with the Monkhorst-Pack grid,[37] and (4 × 4 × 1) Monkhorst-Pack k-point mesh is used. In these calculations, only the two top surface layers were allowed to relax upon geometry optimizations.

The Zr_2Pd_2 cluster binding energies to the MgO(100) surface were calculated according to the following equation:

$$\Delta E_{\text{bind}} = E(\text{slab} + \text{cluster}) - (E(\text{slab}) + E(\text{cluster})) \quad (1)$$

where E(slab + cluster), E(slab), and E(cluster) are the total energies of the cluster on the MgO(100) surface, Zr_2Pd_2/MgO, the clean MgO(100) surface, and the gas-phase cluster Zr_2Pd_2, respectively.

The nudged elastic band (NEB) method[38−40] is applied to locate transition states, and minimum energy pathways are constructed accordingly. The NEB is an efficient method for finding the minimum energy path between the given initial and final states of a transition state.

To compare the dinitrogen hydrogenation process by Zr_2Pd_2 on the MgO(100) surface and in the gas-phase, we also calculate the gas-phase reaction employing the same approach which was applied for the MgO(100) surface studies (the supercell dimensions were taken to be $a = b = c = 30.0$ Å). Below, we compare the energies, ΔE (in kcal/mol), of the dinitrogen hydrogenation reaction by the "naked" and MgO(100) supported Zr_2Pd_2. Cartesian coordinates and energies of all investigated species are given in Supporting Information.

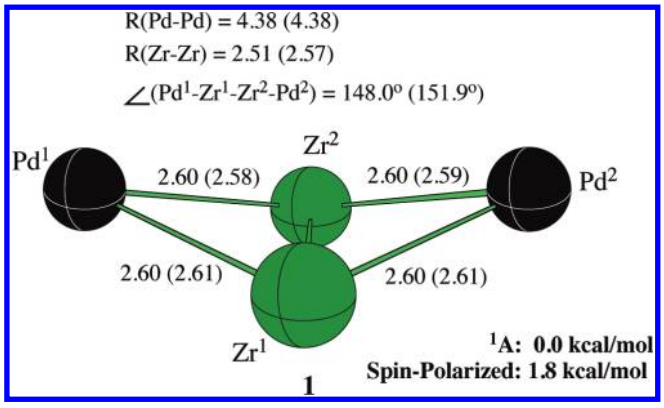

Figure 1. Important geometry parameters of the singlet and spin-polarized (in parentheses) states of the gas-phase Zr_2Pd_2 clusters calculated at the PW91/US-PP level (distances in Å, angles in degree).

To validate our VASP studies, we also studied the gas-phase N_2 hydrogenation reaction using the GAUSSIAN-2003 quantum chemical package.[41] The geometries, vibrational frequencies, and energetics of all intermediates and transition states were calculated using the gradient-corrected PW91 exchange-correlation functional.[42−45] In these calculations, we used the Stuttgart group's pseudopotentials[46] and associated SDD basis sets for transition metal atoms and the standard 6-311 + G(d,p) split-valence basis set for H and N atoms, similar to the previous study.[16] The nature of all calculated intermediates and transition states, as well as reactants and products, was confirmed by performing normal-mode analysis. This approach will be further referred to as "PW91/SDD." Important geometry parameters of all the species studied using this approach, along with their Cartesian coordinates and energies, are given in the Supporting Information.

III. Results and Discussion

III.1. Reactant. (i). "Naked" Zr_2Pd_2 Cluster. Let us first discuss electronic and geometrical structures of the reactant in the gas-phase N_2 hydrogenation, Zr_2Pd_2, **I**. Structure of the Zr_2Pd_2 cluster obtained at the PW91/US-PP level of theory is provided in Figure 1.

As seen from the figure, the "naked" Zr_2Pd_2 cluster favors the "butterfly" structure with the singlet ground state, while its lowest spin-polarized state lies merely 1.8 kcal/mol higher at the PW91/US-PP level. The calculated Zr−Zr, Zr−Pd and Pd−Pd bond distance in the singlet Zr_2Pd_2 are 2.51, 2.60, and 4.38 Å, respectively. In the spin-polarized state, the Zr−Zr bond distance is elongated by 0.06 Å, Zr−Pd distances are changed only slightly, and the Pd−Pd distance remains the same. In the singlet state the dihedral angle ($Pd^1-Zr^1-Zr^2-Pd^2$) is smaller than in the triplet state, 148.0° versus 151.9°. Thus, the Zr−Zr bond converts from the double bond to the single bond upon changing the Zr_2Pd_2 electronic state from the singlet

(21) Bär, M.; Moskaleva, L. M.; Winkler, M.; Reinhard, P.-G.; Rösch, N.; Suraud, E. *Eur. Phys. J. D* **2007**, *45*, 507–514.
(22) Walter, M.; Häkkinen, H. *Phys. Rev. B* **2005**, *72*, 205440.
(23) Del Vito, A.; Sousa, C.; Illas, F.; Pacchioni, G. *J. Chem. Phys.* **2004**, *121*, 7457–7466.
(24) Giordano, L.; Pacchioni, G.; Ferrari, A. M.; Illas, F.; Rösch, N. *Surf. Sci.* **2001**, *473*, 213–226.
(25) Del Vitto, A.; Giordano, L.; Pacchioni, G.; Rösch, N. *Surf. Sci.* **2005**, *575*, 103–114.
(26) Abbet, S.; Ferrari, A. M.; Giordano, L.; Pacchioni, G.; Häkkinen, H.; Landman, U.; Heiz, U. *Surf. Sci.* **2002**, *514*, 249–255.
(27) Neyman, K. M.; Inntam, C.; Matveev, A. V.; Nasluzov, V. A.; Rösch, N. *J. Am. Chem. Soc.* **2005**, *127*, 11652–11660.
(28) Bogicevic, A.; Jennison, D. R. *Surf. Sci. Lett.* **2002**, *515*, L481–L486.
(29) Markovits, A.; Paniagua, J. C.; López, N.; Minot, C.; Illas, F. *Phys. Rev. B* **2003**, *67*, 115417.
(30) Sterrer, M.; Risse, T.; Giordano, L.; Heyde, M.; Nilius, N.; Rust, H.-P.; Pacchioni, G.; Freund, H.-J. *Angew. Chem., Int. Ed.* **2007**, *46*, 8703–8706.
(31) Kresse, G.; Hafner, J. *Phys. Rev. B* **1993**, *48*, 13115–13118.
(32) Kresse, G.; Hafner, J. *Phys. Rev. B* **1994**, *49*, 14251–14269.
(33) Kresse, G.; Furthmüller, J. *Comput. Mater. Sci.* **1996**, *6*, 15–50.
(34) Kresse, G.; Furthmüller, J. *Phys. Rev. B* **1996**, *54*, 11169–11186.
(35) Perdew, J. P.; Wang, Y. *Phys. Rev. B* **1992**, *45*, 13244–13249.
(36) Igel-Mann, G.; Stoll, H.; Preuss, H. *Mol. Phys.* **1988**, *65*, 1321–1328.
(37) Monkhorst, H. J.; Pack, J. D. *Phys. Rev. B* **1976**, *13*, 5188–5192.
(38) Ulitsky, A.; Elber, R. *J. Chem. Phys.* **1990**, *92*, 1510–1511.
(39) Mills, G.; Jónsson, H.; Schenter, G. K. *Surf. Sci.* **1995**, *324*, 305–337.
(40) Henkelman, G.; Uberuaga, B. P.; Jónsson, H. *J. Chem. Phys.* **2000**, *113*, 9901–9904.
(41) Frisch, M. J. et al. *Gaussian 03*, Revision C1; Gaussian, Inc.: Wallingford, CT, 2004.
(42) Perdew, J. P.; Burke, K.; Wang, Y. *Phys. Rev. B* **1996**, *54*, 16533–16539.
(43) Perdew, J. P.; Chevary, J. A.; Vosko, S. H.; Jackson, K. A.; Pederson, M. R.; Singh, D. J.; Fiolhais, C. *Phys. Rev. B* **1992**, *46*, 6671–6687.
(44) Perdew, J. P.; Chevary, J. A.; Vosko, S. H.; Jackson, K. A.; Pederson, M. R.; Singh, D. J.; Fiolhais, C. *Phys. Rev. B* **1993**, *48*, 4978.
(45) Perdew, J. P. In *Electronic Structure of Solids '91*; Ziesche, P., Eschrig, H., Eds.; Akademie Verlag: Berlin, 1991; p 11.
(46) Andrae, D.; Haeussermann, U.; Dolg, M.; Stoll, H.; Preuss, H. *Theor. Chim. Acta* **1990**, *77*, 123.

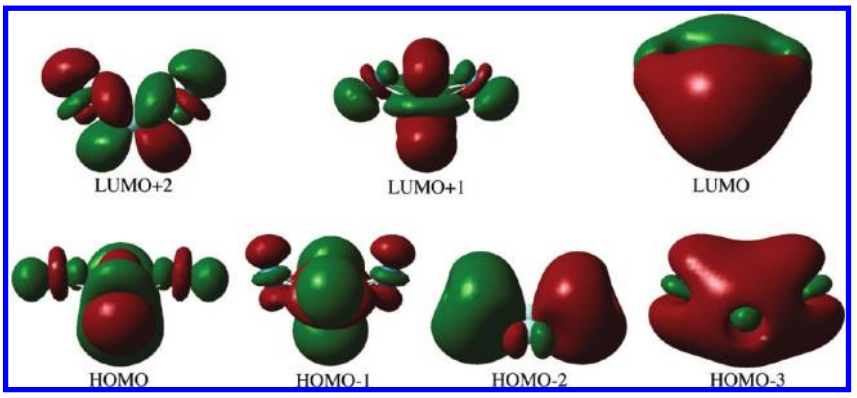

Figure 2. Calculated four HOMOs and three LUMOs of the gas-phase singlet state of the Zr_2Pd_2 cluster.

to the spin-polarized state. The PW91/SDD level studies show similar geometry changes upon going from singlet state to triplet state (see Supporting Information, Figure S1); however, in the case of the PW91/SDD approach, the singlet structure is more flattened in comparison with the triplet (spin-polarized) structure. Also, it is interesting to note, that both approaches gave very similar Zr−Zr and Zr−Pd bond distances and quite similar relative energies of singlet and spin-polarized states of Zr_2Pd_2.

Molecular orbital analysis performed at the PW91/SDD level of theory for the singlet state of Zr_2Pd_2 (Figure 2) shows that its four highest occupied molecular orbitals, HOMO, HOMO-1, HOMO-2, and HOMO-3, have significant contributions from both Zr and Pd atoms. The HOMO could be considered as a bonding combination of d_{z^2}-like atomic orbitals (AOs) of Zr atoms, which have a very small overlap with d_{z^2}-like AOs of Pd atoms. Formally, this MO has Zr−Zr bonding and Zr−Pd antibonding characters. HOMO-1 could be considered as a completely delocalized bonding combination of d_{z^2}-like AOs of all four atoms of the cluster, with a very strong overlap between AOs of Zr atoms and significant overlap along Zr−Pd distances. It also has contributions from s- and d_{yz}-AOs of Zr atoms and s-AOs of Pd atoms. A large part of the electron density is located in the inter-zirconium region. HOMO-2 is responsible for bonding between Zr atoms and antibonding inter actions between Pd atoms of the cluster. It has strong contributions from Zr d_{xy}-AOs and Pd AOs. HOMO-3 could be considered as a combination of s-, d_{z^2}-like, and d_{xz}-orbitals, with predominating contribution from d_{z^2}-like AOs. This orbital is a delocalized MO; however, most of its electron density is shifted toward Pd atoms. As can be seen from Figure 2, all presented lowest unoccupied molecular orbitals (LUMOs) of the free cluster have quite significant contributions from both Zr and Pd atoms.

(ii). MgO(100) Surface. Now, let us consider the second component of the reaction, the intact MgO(100) surface. Magnesium oxide has a rock salt structure like oxides of other alkaline earth metals,[47] and its nonpolar (100) face is by far the most stable surface.[48] The MgO-(100) surface is experimentally well-characterized and is widely used in the chemical industry as a catalyst support.[48−50] Its theoretical description is simplified by the absence of surface reconstructions.[51] Figure 3 shows (a) the model of the MgO(100) surface used in this paper (with two top surface layers relaxed), and (b) the calculated density of states (DOS). The presented DOS is in reasonably good agreement with the results of other theoretical studies:[52] it exhibits a band between −18 and −16 eV because of the 2s orbitals of oxygens and a valence band located between about −5.5 and −1 eV, corresponding to the p-states of oxygen atoms. Also, there is a band between about 2 and 9 eV, which is ascribed to the 3s-states of magnesium atoms. It is interesting to notice that the relaxation of the two surface layers of the model used in our study lowered the energy of the model just by about 0.08 eV (1.75 kcal/mol).

(iii). MgO(100) Supported Zr_2Pd_2 Cluster, Zr_2Pd_2/MgO(100), I/MgO. The PW91/US-PP calculations show that in both singlet and spin-polarized species the **I/MgO** Zr_2Pd_2 favors the butterfly-like structure with Zr atoms coordinated to the surface oxygens (Figure 4a); one should note that the atoms of the lowest two layers of the MgO support, positions of which were not optimized during the calculations, are not shown in this (and following) figures for simplicity of presentation); the spin-polarized structure of **I/MgO** was found to be only 0.5 kcal/mol more stable than the singlet state. In **I/MgO**, Zr−Pd bond distances were found to be the same (2.60 (2.61) Å) for both singlet and spin-polarized species and almost unchanged compared to the gas-phase clusters (cf. Figure 1). Zr−Zr bond distances are significantly elongated in comparison with the free cluster, 2.84 versus 2.51 Å for the singlet state structure, and 2.83 versus 2.57 Å for the spin-polarized structure. Pd−Pd distances,

(47) Wyckoff, R. W. G. *Crystal Structures*, 2nd ed.; Wiley: New York, 1964.
(48) Gibson, A.; Haydock, R.; LaFemina, J. P. *J. Vac. Sci. Technol. A* **1992**, *10*, 2361–2366.
(49) Henry, C. R. *Surf. Sci.* **1998**, *31*, 235–325.
(50) Robach, O.; Renaud, G.; Barbier, A. *Surf. Sci.* **1998**, *401*, 227–235.
(51) See and references therein: (a) Menetrey, M.; Markovits, A.; Minot, C.; Del Vitto, A.; Pacchioni, G. *Surf. Sci.* **2004**, *549*, 294–304. (b) Chiesa, M.; Paganini, M. C.; Giamello, E.; Di Valentin, C.; Pacchioni, G. *Angew. Chem., Int. Ed.* **2003**, *42*, 1759–1761. (c) Dominguez-Ariza, D.; Sousa, C.; Illas, F.; Ricci, D.; Pacchioni, G. *Phys. Rev. B* **2003**, *68*, 054101. (d) Kuzovkov, V. N.; Popov, A. I.; Kotomin, E. A.; Monge, M. A.; Gonzalez, R.; Chen, Y. *Phys. Rev. B* **2001**, *64*, 1–5. (e) Licona, R.; Rivas-Silva, J. F. *Int. J. Quantum Chem.* **2005**, *104*, 919–928. (f) Cárdenas, C.; De Proft, F.; Chamorro, E.; Fuentealba, P.; Geerlings, P. *J. Chem. Phys.* **2008**, *128*, 034708. (g) Chiesa, M.; Giamello, E.; Finazzi, E.; Di Valentin, C.; Pacchioni, G. *J. Am. Chem. Soc.* **2007**, *129*, 10575–10581. (h) Chizallet, C.; Costentin, G.; Che, M.; Delbecq, F.; Suatet, P. *J. Am. Chem. Soc.* **2007**, *129*, 6442–6452.
(52) Xu, Y.-N.; Ching, W. Y. *Phys. Rev. B* **1991**, *43*, 4461–4472.

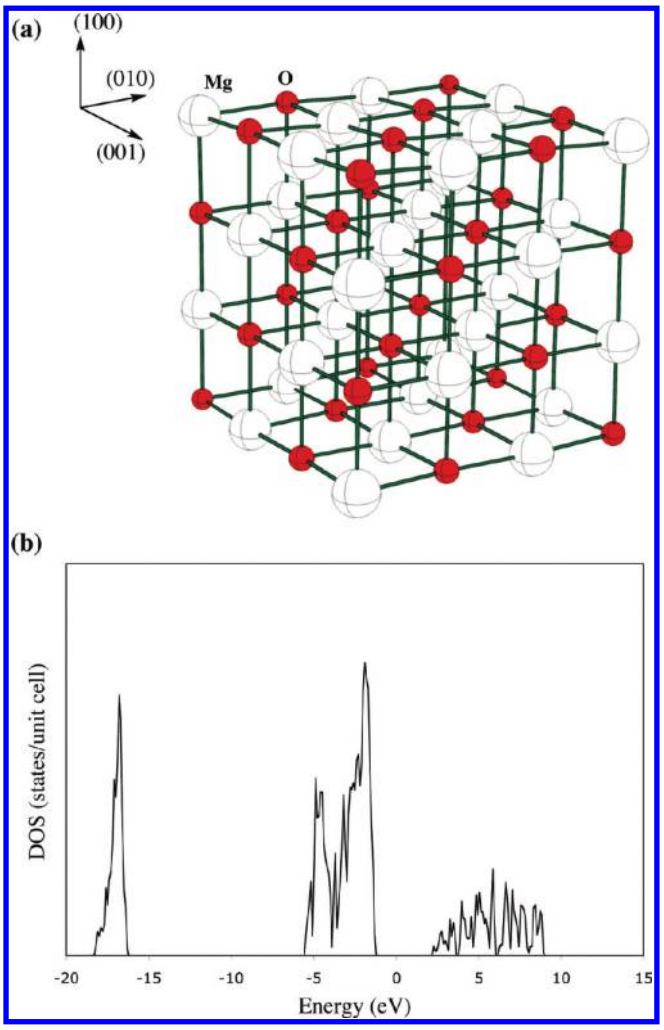

Figure 3. (a) Model of the MgO(100) surface used in the present study, and (b) calculated surface DOS.

however, are shortened by 0.17 Å in the singlet state structure and by 0.15 Å in the spin-polarized structure. The dihedral angle ($Pd^1-Zr^1-Zr^2-Pd^2$) in the singlet state of the supported species increases noticeably compared to the free Zr_2Pd_2 cluster, 157.5° versus 148.0°, but remains almost unchanged for the spin-polarized case, 150.9° versus 151.9°. Thus, the coordination of the Zr_2Pd_2 clusters at the MgO(100) surface leads to noticeable elongation (and weakening) of the Zr−Zr bond and flattens the cluster, too. It is worthwhile to notice large upward shifts of the support atoms because of their interactions with the cluster: oxygens of the first support layer interacting with the zirconium centers of Zr_2Pd_2 move upward by 0.41−0.42 Å, and Mg's interacting with the palladium atoms of Zr_2Pd_2 shift upward by 0.10−0.14 Å. Because of the small energy difference and almost the same geometries of the singlet and spin-polarized species, as well as expected larger stabilization of the singlet state versus the spin-polarized state by interaction with the N_2 molecule, below we will consider only singlet state species.

Comparison of the calculated DOS of **I/MgO** (Figure 4b) with that of the MgO(100) surface (Figure 3b) and free singlet Zr_2Pd_2 species (Figure 4c) shows that the electronic states of the gas-phase Zr_2Pd_2 cluster overlap with the p-states of the MgO(100) surface oxygens; small peaks between 0 and 2.5 eV in the DOS of the supported species could be ascribed to significant surface atoms relaxations.

The binding energies of the Zr_2Pd_2 cluster to the MgO(100) surface are calculated to be quite high, 3.28 eV for the singlet species and 3.30 eV for the spin-polarized species **I/MgO**, using the PW91/US-PP approach. These binding energies are higher compared to those reported for other supported transition metal clusters: 1.95 eV for Pd_3 cluster,[53] and 2.14−2.70 eV for Ni_2-Ni_4 clusters.[54] This could be ascribed to quite strong Zr−O interactions compared to Pd−O or Ni−O bonds. To the best of our knowledge, no theoretical or experimental studies of MgO supported Zr_xPd_y, Zr_xPt_y, or Zr_x clusters have been reported to date. Therefore, comparisons of binding energies should be performed with caution.

Thus, from the above-presented results it can be clearly seen that the MgO supported Zr_2Pd_2 cluster essentially retains its gas-phase "butterfly" geometry and electronic structure, while it binds quite strongly to the surface. This finding of the $Zr_2Pd_2-MgO(100)$ interactions may have a strong impact on the reactivity of the Zr_2Pd_2 cluster, which is considered in detail below.

III.2. Mechanism of Dinitrogen Hydrogenation by Zr_2Pd_2 and Zr_2Pd_2/Mg(100) Clusters. (i). Mechanism of the Gas-Phase Dinitrogen Hydrogenation by Zr_2Pd_2. All calculated intermediates and transition states of the title reaction are presented in Figure 5, and their relative energies are given in Figure 6.

The first step of the reaction is the coordination of N_2 to Zr_2Pd_2, **I**, which produces the intermediate $Zr_2Pd_2(\mu\text{-}1,2\text{-}N_2)$, **II**: this reaction step is found to be exothermic by 55.1 kcal/mol. In **II**, the calculated N−N bond distance is elongated by 0.20 Å compared to the free N_2 molecule (the calculated N−N bond distance is 1.11 Å). Thus, the N−N bond in **II** is significantly activated. The coordination of N_2 to **I** elongates the Zr−Zr bond distance from 2.51 Å, in **I**, to 2.84 Å in **II**. In the next step, the H_2 molecule reacts with the complex **II**, which leads to the H−H bond activation that occurs simultaneously on one of the Zr/N pairs, Zr^1 and N^1 centers, at the transition state **TS1**, and leads to the complex **IV**. In **TS1**, the formed N^1-H^1 bond distance is 1.25 Å and the broken H^1-H^2 bond distance is 1.03 Å. The reaction **II** + $\mathbf{H_2}$ → **IV** is found to occur with a relatively small barrier at **TS1**, 10.1 kcal/mol, and is exothermic by 23.3 kcal/mol. In the resulting complex **IV**, the N−N and Zr−Zr bond distances are elongated by 0.06 Å and 0.17 Å, respectively, compared to **II**. The coordination and activation of the second, third, and fourth H_2 molecules are characterized by continuous elongation of the N−N bond distance (to 1.43, 1.44, and 1.47 Å, respectively, see Figure 5) and lead to the formation of the intermediates **VI**, **VIII**, and **X**, respectively. In **X**, the calculated N−N bond distance is 1.47 Å, just 0.04 Å longer than in the free N_2H_4 molecule (1.43 Å). The addition of the second, third, and fourth H_2 molecules occurs with 8.8, 16.8, and 30.7 kcal/mol barriers at **TS2**, **TS3**, and **TS4**, respectively (Figure 6).

(53) Giordano, L.; Pacchioni, G. *Surf. Sci.* **2005**, *575*, 197–209.
(54) Dong, Y. F.; Wang, S. J.; Mi, Y. Y.; Feng, Y. P.; Huan, A. C. H. *Surf. Sci.* **2006**, *600*, 2154–2162.

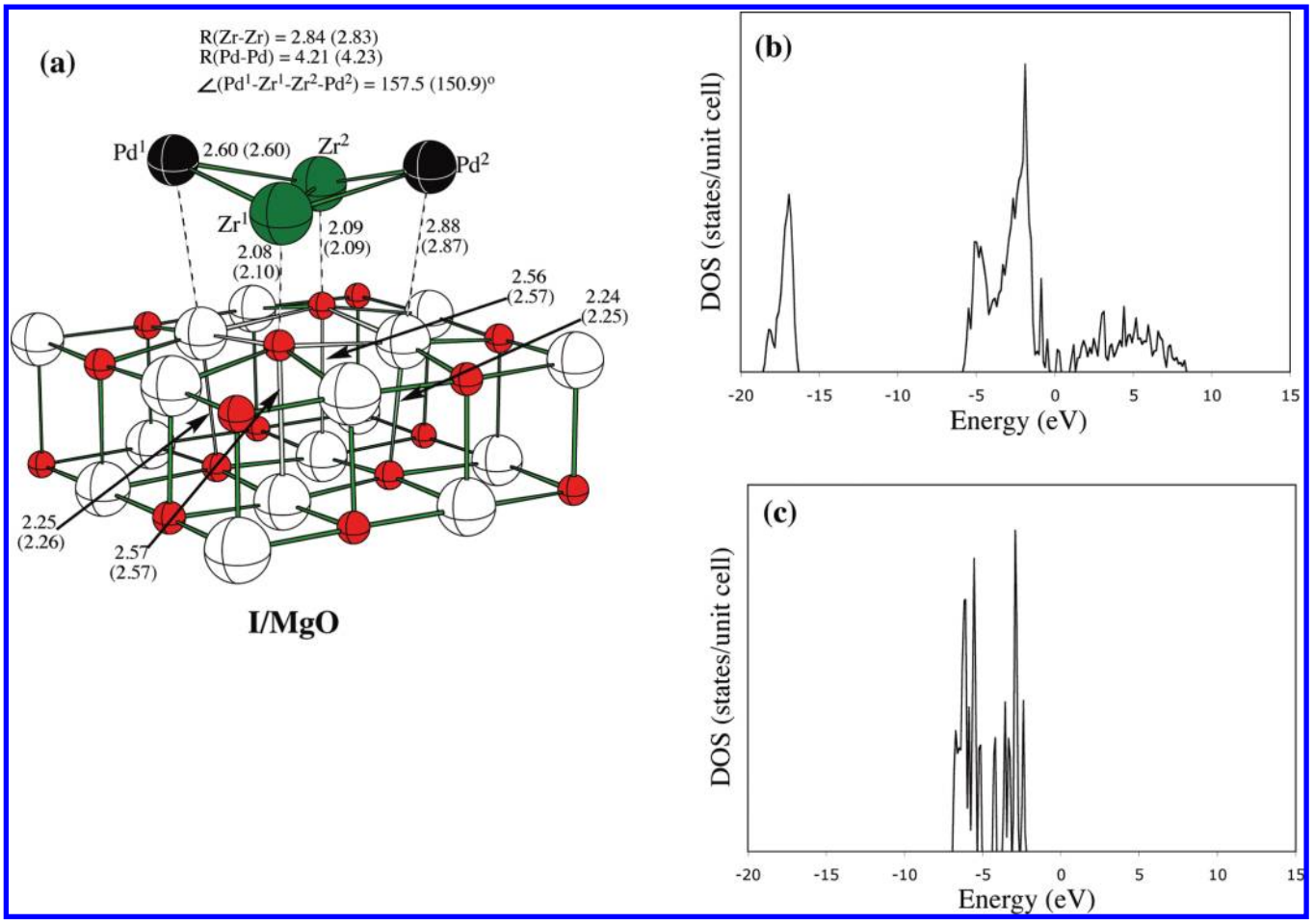

Figure 4. (a) Important geometry parameters of the singlet and spin-polarized (in parentheses) states of the MgO(100) supported Zr_2Pd_2 clusters, and calculated DOS of the supported (b) and "naked" Zr_2Pd_2 cluster at its singlet state (c) (distances in Å, angles in deg.). One should note that the atoms of the lowest two layers of the MgO support are not shown for simplicity of presentation.

The exothermicity of these stepwise reactions, that is, the energy of the reactions **IV** + H_2 → **VI** and **VI** + H_2 → **VIII**, respectively, decreases to −18.2 and −0.1 kcal/mol for the second and third H_2 addition, versus −23.3 kcal/mol for the first H_2 addition. Addition of the fourth H_2 molecule, VIII + H_2 → **X**, is found to be endothermic by 11.4 kcal/mol (Figure 6). The dissociation of the resulting N_2H_4 from the product **X** is endothermic by 26.3 kcal/mol. Thus, the overall reaction $Zr_2Pd_2 + N_2 + 4H_2 \rightarrow (\mu\text{-}1\text{-}H)_2ZrPd_2Zr(\mu\text{-}1\text{-}H)_2 + N_2H_4$, is found to be exothermic by 59.0 kcal/mol, and occurs with a 30.7 kcal/mol rate-determining barrier at **TS4** corresponding to the activation of the fourth H_2 molecule. Since **TS4** is located by 66.0 kcal/mol below the reactants and only about 11 kcal/mol higher than the **II** + H_2 dissociation limit, one may expect that the addition of four hydrogen molecules to N_2 and Zr_2Pd_2 will occur very fast in the gas-phase. Regeneration of the Zr_2Pd_2 from the intermediate **XI** via stepwise H_2 dissociation is calculated to be endothermic by 52.4 kcal/mol: the dissociation of the first H_2 molecule from **XI** to give the $Zr_2Pd_2H_2$ species, **XII**, is endothermic by 28.4 kcal/mol, while the dissociation of the second H_2 molecule from **XII** to regenerate the reactant **I** is endothermic by 24.0 kcal/mol. Thus, the overall gas-phase reaction $Zr_2Pd_2 + N_2 + 4H_2 \rightarrow Zr_2Pd_2 + N_2H_4 + 2H_2$ is calculated to be exothermic by 4.1 kcal/mol. Interestingly, the PW91/SDD calculated energies of the overall reaction of $Zr_2Pd_2 + N_2 + 4H_2 \rightarrow Zr_2Pd_2 + N_2H_4 + 2H_2$ and the geometry parameters of the species involved in this reaction are in reasonable agreement with those obtained at the PW91/US-PP level of theory (see Supporting Information, Figures S1 and S2).

(ii). Mechanism of Dinitrogen Hydrogenation on Zr_2Pd_2/MgO(100), I/MgO. In the study of the mechanism of dinitrogen hydrogenation on Zr_2Pd_2/MgO(100) we follow the same pathway as that obtained for the gas-phase reaction. Thus, the first step of this reaction is the N_2 coordination to the MgO supported Zr_2Pd_2 cluster, **I/MgO**, which leads to the intermediate $Zr_2Pd_2(\mu\text{-}1,2\text{-}N_2)$/MgO, **II/MgO**, given in Figure 7a. Reaction **I/MgO** + N_2 → **II/MgO** is found to be exothermic by 25.6 kcal/mol, that is, the N_2 coordination to the adsorbed Zr_2Pd_2 cluster is by about 30 kcal/mol less favorable than to the "naked" Zr_2Pd_2, **II**. This finding correlates with the calculated N−N bond distance in **II/MgO** and **II**: in the former it is by 0.10 Å shorter than in the latter. In **II/MgO**, the asymmetric character of the Zr−N bonds is observed as well: the Zr^1-N^1 bond distance is 0.05 Å longer than Zr^2-N^2. This indicates the side-on-end-on ($\eta^2;\eta^1$-manner) coordination of N_2 to Zr^1 and Zr^2 centers of **II/MgO**. The similar feature was reported above for the N_2 coordination to the free Zr_2Pd_2. As seen in Figure 7a, in the resulting intermediate **II/MgO**, the Zr−Zr bond distance is significantly shorter (2.62 Å vs 2.84 Å), the $Zr^1-Pd^{1,2}$ and

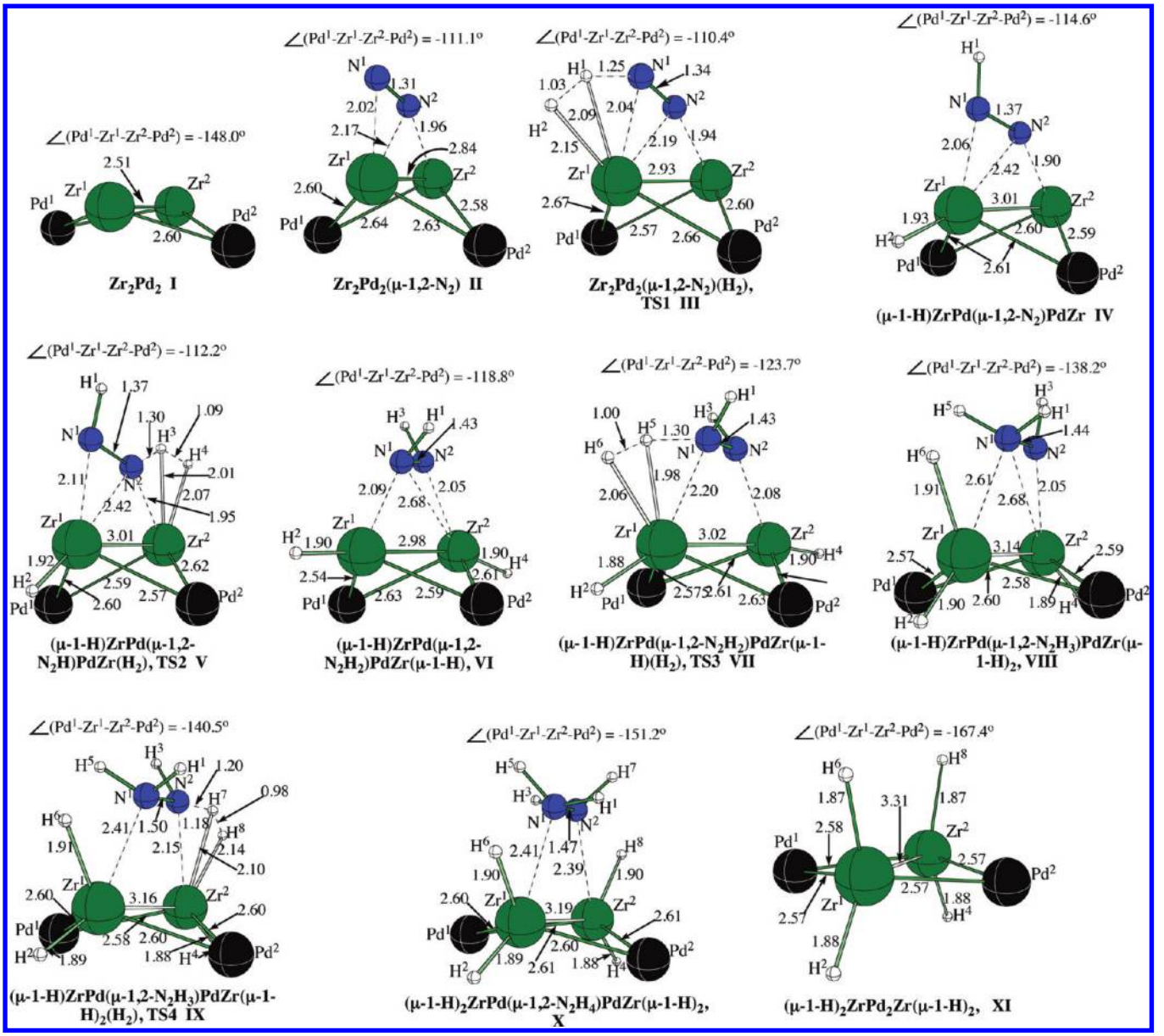

Figure 5. Calculated important geometry parameters (distances in Å, angles in degree) of the reactants, intermediates, and transition states of the gas-phase reaction $Zr_2Pd_2 + N_2 + 4H_2 \rightarrow (\mu\text{-}1\text{-}H)_2ZrPd_2Zr(\mu\text{-}1\text{-}H)_2 + N_2H_4$ studied at the PW91/US-PP level of theory.

$Zr^2-Pd^{1,2}$ bond distances are longer (by 0.13 and 0.06 Å, respectively), the Zr-surface distances are longer (by 0.13−0.21 Å), and the Pd-surface distances are shorter (by 0.19 Å) than in the pre-reaction complex **I/MgO**. Also, it is worthwhile to notice the further flattening of the supported Zr_2Pd_2 cluster and the almost unchanged upward shifts of the ions of the first layer of the MgO support interacting with the cluster atoms (cf. Figures 4 and 7a).

The next step of the reaction is the coordination of the H_2 molecule to **II/MgO** and the activation of the H−H bond via a metathesis transition state **TS1/MgO** (Figure 7b). As seen from the figure, in **TS1/MgO** the broken H−H bond is 1.29 Å, while the formed N^1-H^1, Zr^1-H^2, and Zr^1-H^1 bonds are 1.30 Å, 1.97 Å, and 1.99 Å, respectively. Thus, **TS1/MgO** is a late transition state. Its geometry parameters are in reasonable agreement with those reported above for **TS1** of the gas-phase reaction $Zr_2Pd_2(\mu\text{-}1,2\text{-}N_2) + H_2$ (see Figure 5). Interestingly, the N^1-N^2 bond distance is elongated by just 0.04 Å upon going from **II/MgO** to **TS1/MgO**, and Zr^2-N^2 and Zr^1-Zr^2 bonds are shortened by 0.07 Å and elongated by 0.18 Å, respectively. The H^1-H^2 activation barrier is calculated to be 9.0 kcal/mol versus 10.1 kcal/mol obtained for the gas-phase reaction (see Figure 6).

The product of the H−H bond activation is the MgO supported diazenido-μ-hydride complex (μ-1-H)-ZrPd-(μ-1,2-N_2H)PdZr, **IV/MgO** (Figure 7c). Comparison of the important geometry parameters of **IV/MgO** and **II/MgO** shows that upon hydrogenation of the coordinated N_2 the N^1-N^2 bond distance is elongated by 0.09 Å and the Zr^2-N^2 and Zr^1-N^1 bonds are shortened by 0.09 and 0.10 Å, respectively. The Zr^1-Zr^2 bond distance is elongated by 0.18 Å, while the $Zr^1-Pd^{1,2}$ and $Zr^2-Pd^{1,2}$ bonds are changed only slightly. Also, it is worthwhile to note that among Zr(Pd)-surface distances only the Zr^2-surface distance is shortened noticeably, by 0.08 Å, and the upward shifts of the ions of the first support

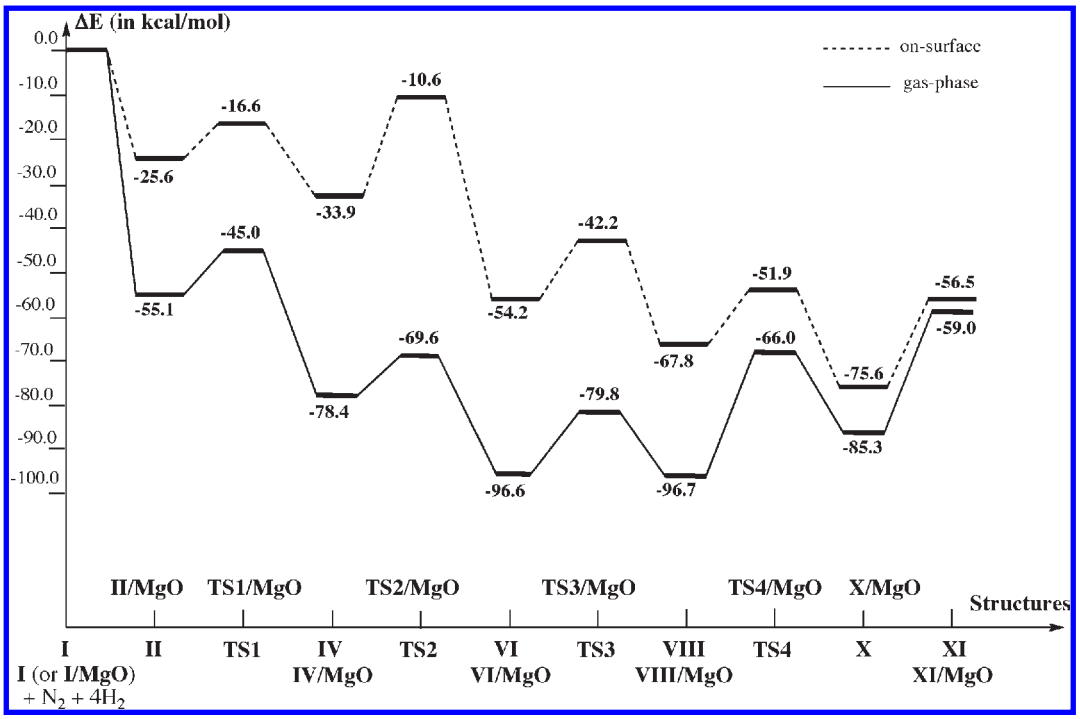

Figure 6. Schematic representation of the potential energy surface (PES) of the reaction $Zr_2Pd_2 + N_2 + 4H_2 \rightarrow (\mu\text{-}1\text{-}H)_2ZrPd_2Zr(\mu\text{-}1\text{-}H)_2 + N_2H_4$ studied in the gas-phase and on the MgO(100) surface with the PW91/US-PP approach.

layer interacting with the cluster remain almost the same. Interestingly, the exothermicity of the reaction **II/MgO** + $H_2 \rightarrow$ **IV/MgO** is calculated to be only 8.3 kcal/mol, which is 15.0 kcal/mol smaller than for the analogous gas-phase reaction. This effect could be explained by additional interactions of Zr-centers (with the surface oxygens) on the MgO surface compared to the "naked" cluster Zr_2Pd_2.

A closer inspection of the transition state **TS1/MgO** (Figure 7b) and the complex **IV/MgO** (Figure 7c) indicates that the H−H bond activation occurs on one of the available Zr/N pairs, like in the gas-phase reaction reported above. Therefore, one may expect that the supported product complex (μ-1-H)ZrPd(μ-1,2-N_2H)PdZr, **IV/MgO**, can also uptake and activate another (second) H_2 molecule on its available Zr^2/N^2 site and form the (μ-1-H)ZrPd(μ-1,2-N_2H_2)PdZr(μ-1-H), **VI/MgO**, product (Figure 8a). The resulting product complex shows the following features: upon the addition of the H_2 molecule the N−N and Zr^1-N^1 bond distances are elongated by 0.14 Å and 0.04 Å, respectively, but the Zr^2-N^2 bond distance is shortened by 0.13 Å. The calculated N−N bond distance in the complex **VI/MgO**, 1.44 Å, indicates the N−N single-bond character. The Zr_2Pd_2 core of the **VI/MgO** is distorted quite significantly, although still preserving its butterfly shape: compared to the **IV/MgO**, the Zr−Zr bond distance is elongated by 0.23 Å, the Pd−Pd distance is shortened by 0.36 Å, and the dihedral angle ($Pd^1-Zr^1-Zr^2-Pd^2$) is changed drastically, from 172.5° in the species **IV** to −155.4°. Interestingly, the Pd-surface distances are changed only very little upon going from **IV/MgO** to **VI/MgO**, but the Zr-surface distances are changed considerably: the Zr^1-surface bond distance is shortened by 0.13 Å, and the Zr^2-surface distance is elongated to 3.50 Å, which implies no bonding at all between the Zr^2 center and the support. Also, it is worthwhile to notice that the H-surface distances are quite long, more than 3.00 Å, implying weak (if any) hydrogen bonding with the support. The exothermicity of the reaction **IV/MgO** + $H_2 \rightarrow$ **VI/MgO** is larger than for the first H_2 addition reaction **II/MgO** + $H_2 \rightarrow$ **IV/MgO**, 20.5 kcal/mol versus 8.3 kcal/mol. This value is close to that found for the gas-phase reaction, 18.2 kcal/mol.

The structure of the transition state **TS2/MgO** (for the second H_2 addition) is given in Figure 7d. As seen from the figure, in **TS2/MgO** the broken H^3-H^4 bond is relatively short, 0.97 Å, while the formed N^2-H^3 and Zr^2-H^4 bonds are 1.30 Å, and 2.01 Å, respectively, which is in reasonable agreement with the structural data found for the gas-phase **TS2** (see Figure 5). Thus, **TS2/MgO** is an early transition state. The activated N−N bond distance is found to be 1.33 Å, which is just 0.03 Å longer than in **IV/MgO**. The Zr^2-N^2 and Zr^1-Zr^2 bonds in **TS2/MgO** are longer by 0.18 Å and 0.03 Å, respectively, than their corresponding values in **IV/MgO**. The H^3-H^4 activation barrier is calculated to be unexpectedly high, 23.3 kcal/mol, versus the 8.8 kcal/mol barrier obtained for the gas-phase reaction (see Figure 6).

Now the question could be raised, if the structure **VI/MgO** is able to add the next two H_2 molecules at mild conditions (with reasonable kinetic and thermodynamic parameters). For this purpose, we have calculated geometry and energy of the MgO supported (μ-1-H_2)-ZrPd(μ-1,2-N_2H_3)PdZr(μ-1-H) and (μ-1-H)$_2$ZrPd(μ-1,2-N_2H_4)PdZr(μ-1-H)$_2$ species, **VIII/MgO** and **X/MgO** (Figures 8c and 9a, respectively), which are products of the third and fourth H_2 addition, respectively. In **VIII/MgO** the N^1-N^2 bond distance is almost the same as in the pre-reaction structure **VI/MgO**, while the Zr^1-N^1 and Zr^2-N^2 bond distances are elongated by 0.09 and 0.32 Å, respectively. The Zr^1-surface distance is shortened by 0.07 Å compared to **VI/MgO**, whereas the

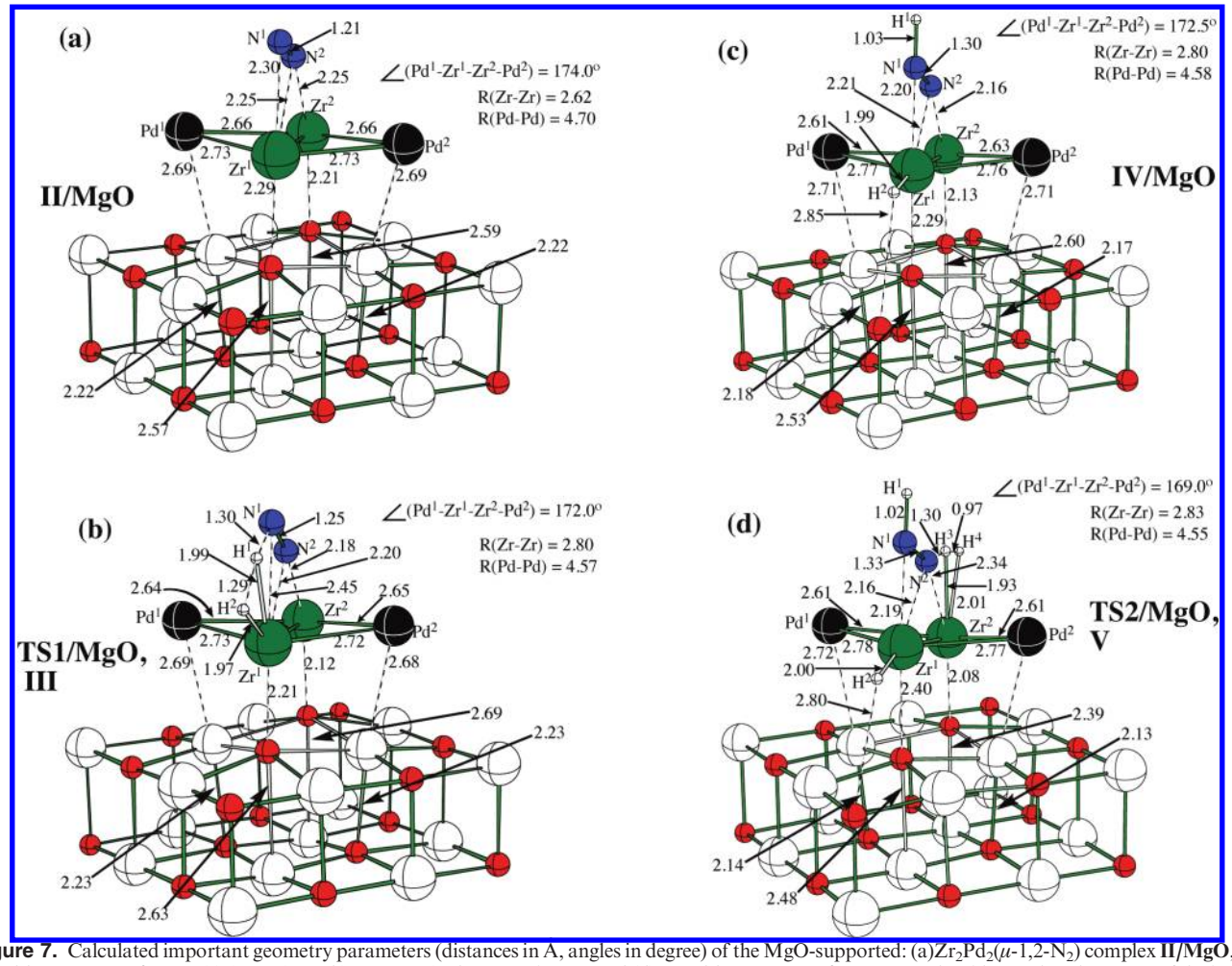

Figure 7. Calculated important geometry parameters (distances in Å, angles in degree) of the MgO-supported: (a)$Zr_2Pd_2(\mu\text{-}1,2\text{-}N_2)$ complex **II/MgO**, (b) transition state **TS1/MgO**, (c) $(\mu\text{-}1\text{-}H)ZrPd(\mu\text{-}1,2\text{-}N_2H)PdZr$ complex **IV**, and (d) transition state **TS2/MgO**. One should note that the atoms of the lowest two layers of the MgO support are not shown for simplicity of presentation.

Zr^2-surface distance is further elongated by 0.22 Å, and $Pd^{1,2}$-surface distances are elongated by 0.12 and 0.04 Å, respectively. The addition of the third H_2 molecule is calculated to have a 12.0 kcal/mol barrier at the transition state **TS3/MgO**, compared with 16.8 kcal/mol reported for the gas-phase reaction (see Figure 6), and is exothermic by 13.6 kcal/mol versus 0.1 kcal/mol found for the similar gas-phase reaction step. The structure of the transition state **TS3/MgO** (for the third H_2 addition) is given in Figure 8b. As seen from the figure, in **TS3/MgO** the broken H^5-H^6 bond is 0.96 Å, while the formed N^2-H^5 and Zr^2-H^6 bonds are 1.35 Å, and 2.13 Å, respectively, which are similar to the values reported for the gas-phase transition state **TS3** (see Figure 5). The N^1-N^2 bond distance is found to be 1.43 Å, only by 0.01 Å shorter than in the pre-reaction complex **VI/MgO**.

The addition of the H_2 molecule to **VIII/MgO** (i.e., the fourth H_2 molecule addition to **I/MgO**) to give the $(\mu\text{-}1\text{-}H)_2ZrPd(\mu\text{-}1,2\text{-}N_2H_4)PdZr(\mu\text{-}1\text{-}H)_2$ species, **X/MgO**, is calculated to be exothermic by 7.8 kcal/mol, while the similar reaction step was reported to be *endothermic* by 11.4 kcal/mol for the gas-phase reaction (see Figure 6). The calculated energy barrier for the on-surface reaction is almost twice smaller than that for the gas-phase reaction, 15.9 versus 30.7 kcal/mol. In the resulting intermediate **X/MgO** the formed N_2H_4 moiety is coordinated to the Zr centers with long Zr−N bond distances, 2.53 and 2.54 Å (Figure 9a): in the gas-phase complex $(\mu\text{-}1\text{-}H)_2ZrPd(\mu\text{-}1,2\text{-}N_2H_4)PdZr(\mu\text{-}1\text{-}H)_2$ these distances are reported to be a similar feature observed which is in reasonable agreement with the corresponding bond distances, 2.43 Å (see Figure 5). The formation of the second N^2-H bond in **X/MgO** causes the shortening of the Zr^2-surface distance: in **X/MgO** it is 2.30 Å, versus 3.72 Å in **VIII/MgO**. The Zr^1-surface distance is elongated by 0.04 Å, and $Pd^{1,2}$-surface distances are shortened by 0.05 and elongated by 0.02 Å, respectively. The above presented geometry parameters indicate that the formed hydrazine molecule should be relatively easily dissociated from the complex **X/MgO** than its gas-phase analogue. Indeed, the calculated energy of the reaction $(\mu\text{-}1\text{-}H)_2ZrPd(\mu\text{-}1,2\text{-}N_2H_4)PdZr(\mu\text{-}1\text{-}H)_2/MgO \rightarrow (\mu\text{-}1\text{-}H)_2ZrPd_2Zr(\mu\text{-}1\text{-}H)_2/MgO + N_2H_4$, 19.1 kcal/mol, is smaller than 26.3 kcal/mol reported for the analogous reaction in the gas-phase (see Figure 6). At the transition state **TS4/MgO**, that connects **X/MgO** with **VIII/MgO** (see Figure 9d), the broken H^7-H^8 bond is 1.12 Å, while the formed N^1-H^7 and Zr^1-H^8 bonds are 1.25 Å and 2.11 Å, respectively, and the N^1-N^2 bond distance is found to be 1.46 Å.

Regeneration of the Zr_2Pd_2 from the intermediate **XI/MgO** via stepwise H_2 dissociation is calculated to be endothermic by 50.5 kcal/mol: the dissociation of the first H_2 molecule from **XI/MgO** to give the $Zr_2Pd_2H_2/MgO$ species, **XII/MgO**, is endothermic by 27.4 kcal/mol,

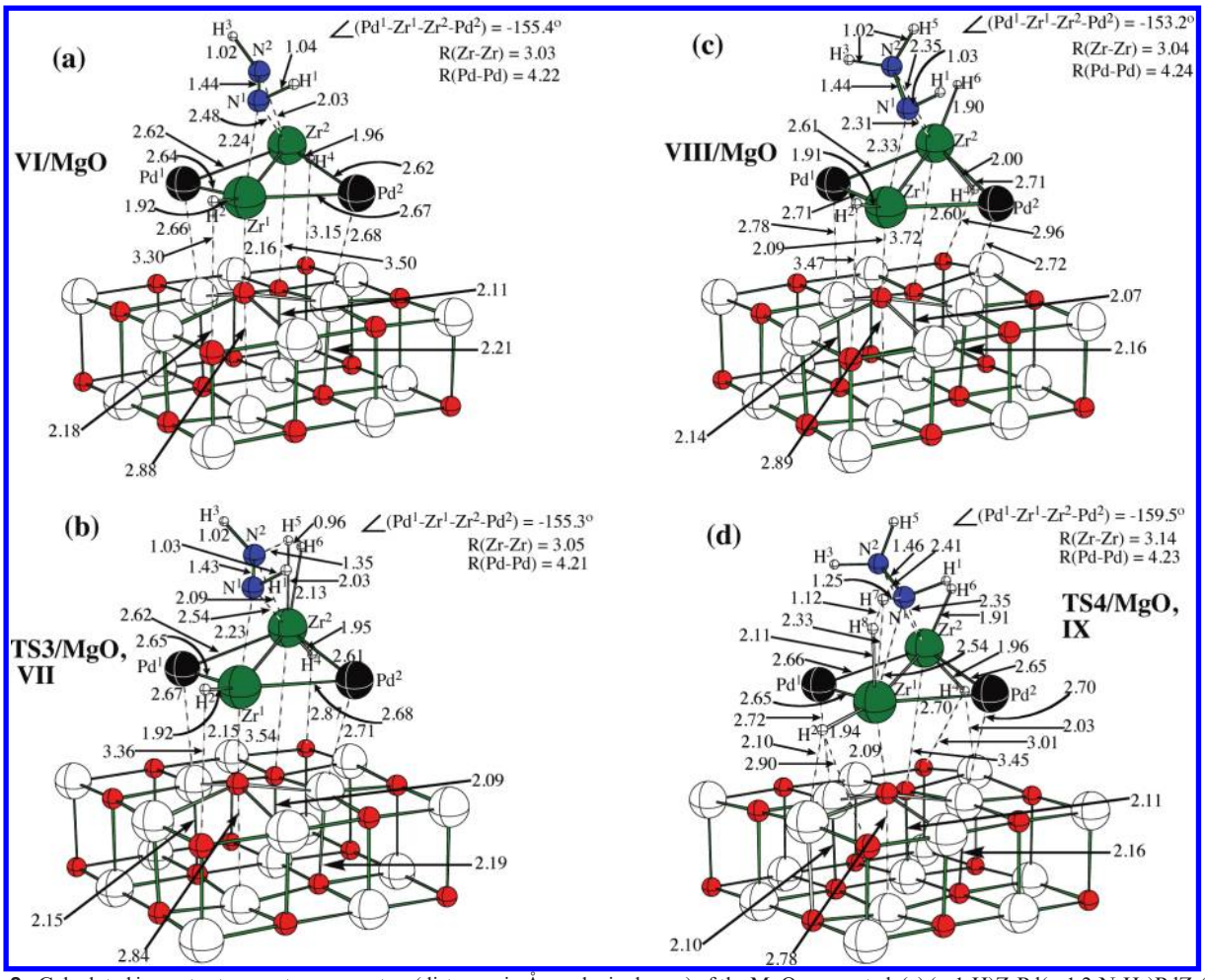

Figure 8. Calculated important geometry parameters (distances in Å, angles in degree) of the MgO-supported: (a) (μ-1-H)ZrPd(μ-1,2-N_2H_2)PdZr(μ-1-H) complex **VI/MgO**, (b) transition state **TS3/MgO**, (c) (μ-1-H_2)ZrPd(μ-1,2-N_2H_3)PdZr(μ-1-H) compound **VIII/MgO**, and (d) transition state **TS4/MgO**. One should note that the atoms of the lowest two layers of the MgO support are not shown for simplicity of presentation.

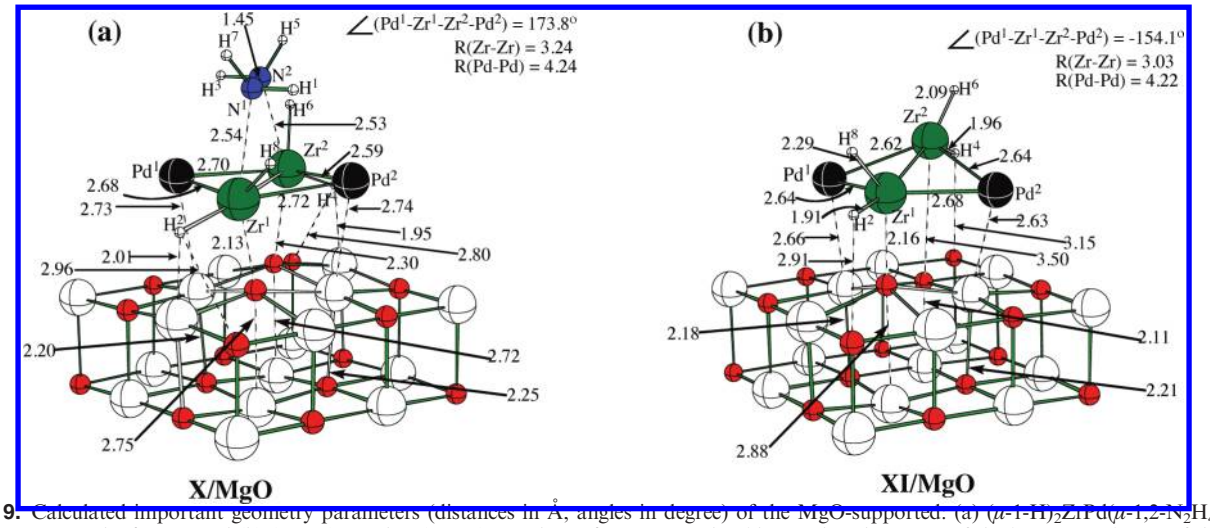

Figure 9. Calculated important geometry parameters (distances in Å, angles in degree) of the MgO-supported: (a) (μ-1-H)$_2$ZrPd(μ-1,2-N_2H_4)PdZr-(μ-1-H)$_2$ compound **X/MgO**, and (b) (μ-1-H)$_2$ZrPd_2Zr(μ-1-H)$_2$ species **XI/MgO**. One should note that the atoms of the lowest two layers of the MgO support are not shown for simplicity of the presentation.

while the dissociation of the second H_2 molecule from **XII/MgO** to regenerate the reactant **I/MgO** is endothermic by 23.1 kcal/mol. Thus, the overall reaction Zr_2Pd_2/MgO + $N_2 + 4H_2 \rightarrow Zr_2Pd_2$/MgO + $N_2H_4 + 2H_2$ is calculated to be exothermic by 6.0 kcal/mol.

In summary, the above presented calculations show that the coordination of N_2 to **I/MgO** is exothermic by 25.6 kcal/mol versus 55.1 kcal/mol reported for the "naked" Zr_2Pd_2 cluster, that is, the bonding energy of N_2 to Zr-centers is almost 30 kcal/mol smaller for the absorbed cluster. This can be explained by interactions between Zr-centers and MgO surface (i.e., an additional bonding to Zr-centers). The addition of the first H_2 molecule to the resulting **II/MgO**, that is, the reaction

II/MgO + H_2 → **IV/MgO**, proceeds with a relatively small, 9.0 kcal/mol, barrier and is exothermic by 8.3 kcal/mol. The same reaction for the "naked" Zr_2Pd_2 cluster requires a slightly larger barrier (10.1 kcal/mol) and is highly exothermic (by 23.3 kcal/mol). Thus, the adsorption of the Zr_2Pd_2 cluster on the MgO(100) surface only slightly increases the H_2 addition barrier to the coordinated N_2 but significantly decreases the exothermicity of the hydrogenation reaction. The addition of the H_2 molecule to the product **IV/MgO** (i.e., the addition of the second H_2 molecule to **II/MgO**) requires a larger energy barrier, 23.3 kcal/mol versus 8.8 kcal/mol for the "naked" cluster, and is exothermic by 20.5 kcal/mol versus 18.2 kcal/mol reported for the "naked" Zr_2Pd_2 cluster. The addition of the H_2 molecule to the **VI/MgO** and **VI** (i.e., the addition of the third H_2 molecule to **II/MgO** and **II**, respectively) requires similar barriers 12.0 versus 16.8 kcal/mol, respectively, but is highly exothermic for adsorbed cluster compared to the "naked" species, 13.6 versus 0.1 kcal/mol. The addition of the fourth H_2 molecule occurs with almost a twice larger barrier for the "naked" than the adsorbed cluster, 30.7 versus 15.9 kcal/mol. Furthermore, this step of the reaction is endothermic (by 11.4 kcal/mol) for the gas-phase cluster, while it is exothermic by 7.8 kcal/mol for the adsorbed cluster. Dissociation of the formed hydrazine molecule from the adsorbed complex **X/MgO** and the "naked" complex **X** requires 19.1 and 26.3 kcal/mol, respectively. *Thus, the presented energetics for the "naked" and MgO supported Zr_2Pd_2 clusters clearly show that adsorption of Zr_2Pd_2 on MgO(100) surface facilitates its reaction with N_2 and four H_2 molecules, as well as formation of hydrazine from the hydrogen and nitrogen molecules.* However, in the "naked" Zr_2Pd_2 cluster the rate-determining step is the fourth H_2 addition (which occurs with a 30.7 kcal/mol barrier at the **TS4**), while for the adsorbed cluster it is the second H_2 addition (which requires a 23.2 barrier at the **TS2/MgO**).

The reported differences in the reactivity of the "naked" and adsorbed Zr_2Pd_2 clusters can be explained by analysis of the nature of H_2 addition in these systems. Indeed, the above presented geometry parameters (specially the N−N and Zr−N bond distances) of the reported intermediates and transition states of the reactions clearly show that the reactions with the first two H_2 molecules are the H−H bond addition to the coordinated N_2 molecule (or N−N bond) and the Zr−N bonds: at the corresponding transition states (**TS1** and **TS2** for the gas-phase process, and **TS1/MgO** and **TS2/MgO** for the on-surface reaction) the H−H and N−N bonds are broken (or partially broken) simultaneously. For the gas-phase reaction, the involved Zr−N bonds are elongated but for the on-surface reaction, those bonds are shortened because of different ligand environments. Indeed, during these reactions the N−N bond elongates from 1.21 Å (in **II/MgO**) to 1.30 Å (in **IV/MgO**) and to 1.44 Å (in **VI/MgO**) for the on-surface reaction and from 1.31 Å (in **II**) to 1.37 Å (in **IV**) and 1.43 Å (in **VI**) for the gas-phase reaction. In contrast, the last two H_2 additions (third and fourth) are mainly H−H activation between the corresponding Zr- and N-centers (i.e., H−H addition to the Zr−N bonds): indeed, during these reactions the N−N bond distance remains the same, while Zr−N bond elongates significantly. Since the Zr−N bonds of the pre-reaction complexes (**VI** and **VIII**, for gas-phase reactions, and **VI/MgO** and **VIII/MgO**, for the on-surface reaction) are much stronger in the "naked" than in adsorbed cluster, one should expect these steps to be relatively more demanding for the former than latter.

IV. Conclusions

The following conclusion can be made from the above-presented data.

(1) Adsorption of the Zr_2Pd_2 cluster on the MgO(100) surface mostly retains its gas-phase geometry. While the DOS analysis suggests strong mixing of electronic states of the MgO support and Zr_2Pd_2 cluster, the electronic structure of the supported cluster is found to be similar to that of its gas-phase counterpart.

(2) Adsorption of the Zr_2Pd_2 cluster on the MgO(100) support facilitates its reaction with nitrogen and four hydrogen molecules to produce hydrazine, that is, $Zr_2Pd_2/MgO + N_2 + 4H_2 \rightarrow (\mu\text{-}1\text{-}H)_2\text{-}ZrPd_2Zr(\mu\text{-}1\text{-}H)_2/MgO + N_2H_4$. The first step of the reaction, the N_2 coordination to the cluster, is found to be approximately 30 kcal/mol less exothermic for MgO-supported than gas-phase cluster. The rate-determining step of the studied reactions is the fourth H_2 addition (which occurs with a 30.7 kcal/mol barrier at the **TS4**), for the "naked" Zr_2Pd_2 cluster, and the second H_2 addition (which requires a 23.2 barrier at the **TS2/MgO**) for the MgO-adsorbed cluster.

(3) The reactions of the resulting N_2-complexes of the "naked" and MgO-supported Zr_2Pd_2 clusters with the first two H_2 molecules are the H−H bond addition to the coordinated N_2 molecule. In contrast, last two H_2 additions (the reaction with the third and fourth H_2 molecules) are mainly H−H bond activation between the corresponding Zr- and N-centers (i.e., the H−H addition to the Zr−N bonds) of the pre-reaction complexes.

Thus, on the basis of the results reported here one may conclude that the embedding of free clusters of transition metals on the MgO(100) surface is a very promising approach that opens a way to utilize the high catalytic activity of these nano-scaled clusters. Here, we predicted that the Zr_2Pd_2/MgO(100) cluster can be an efficient catalyst for direct hydrogenation of the nitrogen molecule.

Acknowledgment. The use of computational resources at the Cherry Emerson Center for Scientific Computation is also acknowledged.

Supporting Information Available: (1) Completed ref 41, (2) Cartesian coordinates along with energies for all species studied both in the gas-phase (Table S1) and on-surface reactions (Table S2), and (3) important geometry parameters of the reactants, intermediates, and transition states of the gas-phase reaction $Zr_2Pd_2 + N_2 + 4H_2 \rightarrow (\mu\text{-}1\text{-}H)_2ZrPd_2Zr(\mu\text{-}1\text{-}H)_2 + N_2H_4$ calculated at the PW91/SDD level. This material is available free of charge via the Internet at http://pubs.acs.org.